NACA RM A52A14b

NACA

RESEARCH MEMORANDUM

EXPERIMENTAL INVESTIGATION OF THE DRAG OF 30°, 60°, AND 90° CONE CYLINDERS AT MACH NUMBERS BETWEEN 1.5 AND 8.2

By Alvin Seiff and Simon C. Sommer

Ames Aeronautical Laboratory
Moffett Field, Calif.

NATIONAL ADVISORY COMMITTEE
FOR AERONAUTICS
WASHINGTON

April 25, 1952
Declassified December 7, 1953.

NATIONAL ADVISORY COMMITTEE FOR AERONAUTICS

RESEARCH MEMORANDUM

EXPERIMENTAL INVESTIGATION OF THE DRAG OF 30°, 60°, AND 90° CONE CYLINDERS AT MACH NUMBERS BETWEEN 1.5 AND 8.2

By Alvin Seiff and Simon C. Sommer

SUMMARY

The total drag coefficients of 60° cone cylinders of fineness ratio 2.07 were measured in free flight at Mach numbers from 1.5 to 8.2. Drag measurements also were made for 30° and 90° cone cylinders with fineness ratios of 3.07 and 1.70, respectively, at Mach numbers between 1.5 and 3.5. The Reynolds numbers based on model length were between 0.3 and 2.4 million.

It was concluded that the Taylor and Maccoll theory for the wave drag of cones is accurate for the 60° cone over the entire range of Mach numbers from 2 to 8. (No imperfect gas effects were encountered in these tests.) In the narrow range of Mach numbers greater than that of wave detachment but less than that for which the flow is everywhere supersonic, the Taylor and Maccoll theory for the wave drag of the 90° cone was found to be subject to question. The variation with Mach number of the base drag of the 60° cone cylinder was estimated from the total drag measurements at Mach numbers between 2 and 4.5.

At high supersonic Mach numbers, discontinuity lines along the outermost streamline of the conical flow region were recorded in the shadowgraph pictures of the cone cylinders. A study of these discontinuities indicated that they were simple discontinuities in density gradient, that they did not influence the drag, and that they did not represent a basically new flow effect.

INTRODUCTION

The development of test equipment for aerodynamic research at Mach numbers above 4 is receiving considerable attention at the present time but has not yet progressed to where very much aerodynamic data is

available for these speeds. One new facility which has been developed primarily for research at high supersonic Mach numbers is the Ames supersonic free-flight wind tunnel (reference 1). The tests described in this report were the first conducted in this wind tunnel.

The purpose of these tests was to study the drag characteristics at high supersonic Mach number of three short cone cylinders with 30°, 60°, and 90° total cone angles. The drag of these models is due to three separate effects. The largest part, because of the large cone angles, is due to high pressures on the surface of the cone and is referred to in this report as the wave drag of the cone. The second largest part is the base drag. The third part, the skin friction, is a small fraction of the total drag. Since the total drag characteristics can be understood only through an understanding of the characteristics of the drag components, it was a primary purpose of this work to interpret the experimental results in terms of the drag components. Because of the predominance of the wave drag, it was possible to estimate it reliably from the experiment and to draw conclusions regarding the accuracy of the Taylor and Maccoll theory over the entire range of Mach numbers. It was more difficult to obtain reliable base-drag data but an indication of the dependence of base drag on Mach number for a laminar boundary layer of nearly constant thickness was obtained for Mach numbers up to 4.5 and is presented.

SYMBOLS

A frontal area of model, square feet

C_D total drag coefficient $\left(\frac{\text{drag force}}{q_o A}\right)$

C_{D_b} base drag coefficient $\left(\frac{p_o - p_b}{q_o}\right)$

$C_{D_{b_{max}}}$ maximum possible base drag coefficient, corresponding to zero pressure at the model base

C_{D_b}' modified base drag coefficient $\left(\frac{p' - p_b}{q'}\right)$

C_{D_f} skin-friction drag coefficient $\left(\frac{\text{skin-friction drag}}{q_o A}\right)$

C_{D_w} wave drag coefficient $\left(\frac{\text{wave drag of cone}}{q_o A}\right)$

d body diameter, feet

H_r reservoir pressure of wind tunnel, atmospheres

M Mach number

p static pressure, pounds per square foot

p_b base pressure, pounds per square foot

q dynamic pressure, pounds per square foot

R Reynolds number based on body length and free-stream conditions

V air velocity in boundary layer relative to model, feet per second

δ boundary-layer thickness, feet

Subscripts and Superscripts

o free-stream conditions, relative to model

δ conditions just outside the boundary layer

' conditions in vicinity of base (See footnote 2, p. 7.)

DESCRIPTION OF TESTS

In the Ames supersonic free-flight wind tunnel, research models are fired at high speed through an 18-foot-long test section in a direction opposite to the wind-tunnel air stream which has a Mach number of 2. High supersonic Mach numbers can be reached in this way. The Mach number can be varied by changing the model launching velocity. The Reynolds number can be varied by changing the wind-tunnel reservoir pressure. The wind tunnel can also be used for low supersonic Mach numbers by launching the models through still air (referred to in this report as "air off") for which case the Reynolds number is fixed by the model size and the Mach number.

In these tests, the models were launched from a 220 Swift sporting rifle mounted in the wind-tunnel diffuser. They were spin stabilized and were therefore limited to short length. Cone cylinders with 30°, 60°, and 90° total cone angles and cylinders of fineness ratio 1.2 were

tested. The main results were obtained with 60° cone cylinders rather than with the more aerodynamically desirable 30° cone cylinders because the stability of the 30° cone cylinder would not permit its use over the full range of test conditions. About half of the 60° cone cylinders were launched in sabots as shown in figure 1(a) to prevent marring of the model surface. The sabots were fractured by the firing impact and fell off the model after emerging from the muzzle. The remainder of the models (tested earlier) were fired without sabots (fig. 1(b)) and were marked on the cylindrical surface by the rifling of the gun. There were 6 rifling grooves about 0.4 as wide as the lands between them, about 1 percent of the diameter deep, and helical to the extent of one turn in 14 inches of advance.

The smooth 60° cone cylinders were tested at Mach numbers from 1.5 through 8.2 at the Reynolds numbers based on length indicated in figure 2. Spin stability limitations made it necessary to restrict the tests to the minimum reservoir pressure at Mach number 5 and also prevented use of the maximum available reservoir pressure at Mach numbers 7 and 8. The rifled 60° models were tested at Mach numbers from 1.5 to 6.9 and at Reynolds numbers 12 percent greater than those in figure 2. The 30° cone cylinders were restricted by their stability to air-off use at Mach numbers between 1.5 and 3.7. The 90° cone cylinders were arbitrarily restricted to air-off use.

Drag coefficients of these models were measured by recording the time-distance histories of their flights through the test section. Four shadowgraph stations and a chronograph provide the record from which deceleration and drag coefficient can be computed. With four stations, four independent values of the drag coefficient can be obtained. The average total scatter of the four independent values was 2.8 percent for the smooth 60° cone cylinder. The four values were averaged to obtain a single data point for each round fired. In a plot of drag coefficient as a function of Mach number for the smooth 60° cone cylinder, the mean deviation of the 32 data points from the faired curve was 1.2 percent with a maximum deviation of 3.8 percent.

RESULTS AND DISCUSSION

Smooth 60° Cone Cylinder

The measurements of total drag coefficient for the smooth 60° cone cylinders are plotted in figure 3 as a function of free-stream Mach number. A large number of measurements was made to investigate the experimental scatter in the new wind tunnel. The clusters of points at Mach numbers 7 and 8 include points of varying Reynolds number, between 1.1 and 2.4 million. Individual models having more than 3°

projected angle of attack in any shadowgraph station were rejected and are not included in the figure. The increment in wave drag due to 3° angle of attack was estimated theoretically to be less than 1 percent.

Shadowgraph pictures of three of these models, at Mach numbers 1.71, 4.49, and 8.14 are reproduced in figure 4. There is optical distortion in these pictures due to strong density gradients in the flow close to the model. At high Mach numbers, the light deflection in the conical shock wave is of such a magnitude that the region between the wave and the cone is as dark as the model shadow and appears to be an extension of the model. The light deflection in the expansion at the shoulder is sufficient to cut across the bow wave, giving the appearance of a break in the wave. The weak shock waves which originate on the cylinder near the cone are believed due to reattachment of the flow after separation at the corner. The light refraction in this vicinity causes the models to appear swollen at the shoulder. That they were not actually deformed in this way was shown by examination of large numbers of recovered models.

Comparison with theory of Taylor and Maccoll.- The data of figure 3 were used to estimate the wave drag of the cone at Mach numbers 2, 5, and 8. The procedure was to subtract the estimated base drag and skin friction from the total drag. This procedure was inherently accurate because the base drag and skin-friction drag were only small parts of the total drag. At Mach numbers 5 and 8, the base drag was arbitrarily chosen to be 0.7 of that corresponding to a vacuum at the base. The error in estimating wave drag due to this arbitrary choice would be limited to 2 percent at Mach number 5 and 1 percent at Mach number 8 if the actual base drag were between 0.5 and 0.9 of the maximum possible. At Mach number 2, the base drag was obtained from wind-tunnel measurements of the base pressure of this model made in the Ames 1- by 3-foot supersonic wind tunnel No. 1. The skin friction was estimated by the boundary-layer-momentum method (see appendix) because of the major differences between a 60° cone cylinder and a flat plate. In these calculations, the boundary layers were assumed fully laminar because of the low Reynolds numbers and because of the appearance of the flow behind the base in the shadowgraph pictures.[1] The calculated

[1] After flowing off the body, the boundary layer follows the outside boundary of the dead-air region behind the body. For Reynolds numbers at which laminar flow might be expected, a fairly sharp line occurs at this boundary as in figure 4. For Reynolds numbers at which turbulent boundary-layer flow might be expected, the boundary is very diffuse and indefinite. The association of the appearance of this line with the type of boundary-layer flow has been confirmed in a large number of tests as yet unreported and is taken to be a strong indication of the existence of laminar boundary layers in the present case.

skin-friction drag coefficients were found to be never greater than 1.5 percent of the total drag.

A comparison of the wave drag coefficients estimated from the experiment with those given by the theory of Taylor and Maccoll (taken from reference 2) is presented in figure 5. The difference is nowhere greater than 2.1 percent. It is important to note that in these tests the local temperatures and pressures were within the range of application of the perfect gas law.

Base drag.- In the preceding discussion of wave drag, it was shown that the theoretical wave drag was correct within the accuracy of the experiment. This conclusion was reached using experimental base-pressure data at Mach number 2 and arbitrary choice of base drag at the higher Mach numbers and it was shown that the arbitrariness of this choice did not affect the conclusion drawn. In this section, it will be assumed that the theoretical wave drag correctly represents the experiment within 1 percent at all Mach numbers and this assumption will be used to estimate the variation with Mach number of the base drag of the 60° cone cylinder. The procedure is to subtract the theoretical wave drag and the calculated skin-friction drag from the total drag curve of figure 3. The results of this operation are shown for Mach numbers up to 4.5 in figure 6. The base drag coefficient obtained in the Ames 1- by 3-foot supersonic wind tunnel for this same model is plotted in the figure for comparison. The estimated limits of uncertainty of the base drag curve are indicated by dashed lines. These limits were calculated by allowing ±0.008 error in total drag coefficient (the root-mean-square deviation of the data points from the faired curve for the air-off tests), ±0.006 error in the theoretical wave drag coefficient (±1 percent), and ±0.002 error in the skin-friction drag coefficient (±25 percent). These errors were applied cumulatively and as such are believed to be a liberal allowance for error. It is apparent that the uncertainty become excessive in the right half of the figure.

The effect of the varying test Reynolds numbers on the base drag curve was examined in terms of the theory of reference 3 in which the boundary-layer thickness was proposed as the significant boundary-layer parameter for base drag. The boundary-layer thicknesses were calculated and found to be nearly constant, δ/d ranging from 0.0092 to 0.0105. Therefore the curve of figure 6 shows the Mach number effect at a nearly constant value of boundary-layer thickness.

In order to make the data of figure 6 applicable to other body shapes, the modification described in reference 3 was applied. This consists of changing the reference conditions for the base drag coefficient from those of the free stream to those in the vicinity of

the base.[2] The modified base-drag data are plotted in figure 7. Within the limitation of this method of correlation, the data of figure 7 should be applicable to bodies of any shape for Mach numbers in the vicinity of the base corresponding to those in the figure and for laminar boundary layers with $\delta/d = 0.01$.

Effect of Reynolds number.- The effect of Reynolds number on the drag was investigated at a Mach number of 8 and at Reynolds numbers between 1.0 and 2.4 million. Within this range, the change in drag coefficient was smaller than the experimental scatter, as is shown in figure 8. The smallness of the effect is due to the fact that the viscous drag components are only a small fraction of the total drag. Furthermore, the effects of Reynolds number variation on the base drag and skin-friction drag tend to compensate.

Rifled Models

Effect of rifling.- The effect of rifling on the drag was investigated by comparing the test results of the rifled 60° cone cylinder with those of the smooth 60° cone cylinder. In figure 9, the measured drag coefficients of the rifled model are plotted as a function of Mach number and are compared with the drag curve of the smooth model from figure 3. The comparison shows that the drag coefficient of the rifled model was about 2.3 percent higher than that of the smooth model below a Mach number of 2.5 and about 6 percent higher at Mach numbers from 2.5 to 7.0. The sudden change that occurred at Mach number 2.5 was apparently due to the occurrence of boundary-layer transition on the rifled models above this Mach number. This is indicated by the shadowgraph pictures. (See figs. 10 and 4 and footnote 1.)

Applicability of the conical-wave-drag theory near wave detachment.- The measured drag coefficients for the 30° and 90° cone cylinders are plotted as a function of Mach number in figure 11 along with the theoretical wave-drag curves. Shadowgraph pictures of these models appear in figure 12.

The maximum drag coefficient of the 90° cone cylinder occurred near the Mach number of shock detachment, 2.38. Near this Mach number, the experimental total drag curve and the theoretical wave-drag curve are very dissimilar. Considered together, they indicate that the combined base drag and skin-friction drag decrease from 60 percent $C_{D_{b_{max}}}$

[2]Conditions in the vicinity of the base are defined as those at the middle of a hypothetical cylinder, extended behind the actual body to the end of the dead-air region. The numerical values for pressures at this location were taken from reference 4.

at Mach number 2.6 to 16 percent at Mach number 2.38. The sudden large decrease in base drag seems very improbable and is not supported by the shadowgraph pictures which show that the flow off the body at a Mach number of 2.39 is still sharply convergent and comparable to that behind a 30° cone cylinder at about the same Mach number (figs. 12(c) and (d)), suggesting that the base drag is normal. A more reasonable explanation for the dissimilarity of the two curves is given in the introduction of reference 2 where it is pointed out that the theory of Taylor and Maccoll might give erroneous results at Mach numbers just above that of shock attachment when applied to cones of finite length. Just above the Mach number of shock attachment, the conical flow is fully subsonic. In this situation, the expansion region at the base of the cone can act to reduce the pressures on the cone and thus reduce the actual wave drag below the theoretical. The theory predicts subsonic conical flow about a 90° cone at Mach numbers between 2.38 and 2.62 and this is the range where the inconsistency exists. Partially subsonic conical flow persists up to a Mach number of 2.80 but, in this range, the inconsistency is either small or zero and its existence cannot be proved in the present experiments. The curves of figure 11(a) suggest that the hypothesis of reference 2 is correct at Mach numbers for which the theory predicts fully subsonic conical flow.

The data for the 30° cone cylinder were qualitatively consistent with the Taylor and Maccoll theory and with the other drag measurements. No quantitative use was made of these data because of the uncertainty introduced by the rifling.

The Discontinuity Lines in the Shadowgraph Pictures

At high supersonic Mach numbers, the shadowgraph pictures of many of these cone cylinders contain unusual lines of discontinuity. These lines appear to originate at the bow shock wave near the body and to lie along a streamline in the region behind the shock wave. Figures 4(b), 10(b), 10(c), 12(e), and 12(f) are shadowgraphs containing these lines. It is evident that the lines are present with both the rifled and the smooth models, but that they are different in character, being periodic with the rifled models (e.g., fig. 10(b)) and steady with the smooth (e.g., fig. 4(b)). The period associated with the rifled models can be correlated to the rate of spin and the number of grooves.

The shadowgraph pictures containing these lines and the experimental conditions influencing their formation were studied. It was concluded that the lines originate at the point where the fan of expansion waves produced by the cone-cylinder junction first intersects the bow shock wave. In order to further study the formation of these lines, the flow

about the 60° cone cylinder was analyzed by the method of characteristics at a free-stream Mach number of 5.01. This analysis showed that the density gradient changed abruptly across one streamline in the flow field. This streamline passed through the intersection of the bow shock wave and the first expansion wave from the cone-cylinder junction. The abrupt change in density gradient produces the lines in the shadowgraph pictures.

In simple physical terms, the explanation for the discontinuity in density gradient is that, for those streamlines which pass through the conical-flow region, the stagnation density just downstream of the bow shock wave is the same on every streamline; but, for those streamlines which pass through the highly curved bow shock wave just outside the conical-flow region, the stagnation density differs considerably on adjacent streamlines. The streamline which separates the two regions is therefore the locus of a discontinuity in density gradient.

This explanation of the origin of the discontinuity lines indicates that they are not important to the drag or other forces. Instead, they overemphasize the existence of what is only an interesting detail of the flow about cone cylinders.

CONCLUSIONS

1. The theoretical wave drag of the 60° cone, as predicted from the theory of Taylor and Maccoll, was found to be correct within the accuracy of the experiments over the entire Mach number range from 2 to 8. The temperature and pressure conditions of this test were never outside the range of the perfect gas law.

2. In the narrow range of Mach numbers greater than that of wave detachment but less than that for which the flow is everywhere supersonic, the Taylor and Maccoll theory for the wave drag of a 90° cone of finite length was found to be subject to question.

3. Unusual discontinuity lines were observed in the flow about the cone cylinders at high supersonic Mach numbers. These were found to be simple discontinuities in density gradient across the outermost streamline of the conical-flow region. They did not represent a basically new flow effect nor did they influence the drag.

Ames Aeronautical Laboratory,
National Advisory Committee for Aeronautics,
Moffett Field, Calif.

APPENDIX

CALCULATION OF THE SKIN-FRICTION DRAG AND THE BOUNDARY-LAYER THICKNESS

The skin-friction drag and boundary-layer thickness for laminar flow over the 60° cone cylinder were estimated using the von Kármán momentum method. Since this type of calculation is well known, it will not be explained in detail here. In the following paragraphs, only the main features and assumptions of these particular calculations will be discussed.

The basic equation used was that given in reference 5 for compressible boundary-layer flow with pressure gradient on a body of revolution at zero angle of attack. It was derived in the reference by applying Newton's second law of motion to the shear and pressure forces and the momentum changes in the boundary layer.

In applying this equation, it was assumed that the nondimensional velocity and density profiles were invariant along the body. The velocity profile was modeled after those determined theoretically for a flat plate in references 6 and 7. These profiles can be reasonably approximated at high supersonic Mach numbers by a straight line out to $V = 0.9V_\delta$ for cases with or without heat transfer. The density profiles were estimated with the aid of equation 4, reference 6, which assumes the Prandtl number is 1. The boundary-layer thickness was defined as the distance from the body to the point where $V = 0.9V_\delta$.

The model surface was assumed to remain at room temperature during its flight through the test section.[3] This assumption was made as a result of calculations which showed that, in the short time of flight, the amount of heat transferred through the boundary layer was small compared to the heat capacity of the model. Temperature gradients within the model were also calculated and found to be small.

The small pressure and velocity gradients along the cylinder of the model were not taken into account because it was felt that the changes in the skin friction would be too small to justify the added complication. Mean values of pressure and velocity were used instead.

The behavior of the boundary layer in expanding around the corner from the cone onto the cylinder was analyzed on the basis of two assumptions: (1) that the mass flow of the boundary-layer air was the same

[3]The temperature of the model surface must be known because this temperature determines the viscosity at the wall (hence the local shear) and also affects the density distribution and the boundary-layer thickness.

at a point on the cylinder just beyond the corner as at a point on the cone just ahead of the corner; (2) that the nondimensional velocity and density profiles were unaffected by the expansion. The latter assumption is known to be inaccurate, but it greatly simplified the calculation and is not believed to have introduced a serious error in terms of the accuracy required.

With the density and velocity profiles and the mass flow of the boundary layer assumed unchanged, the only effect of the expansion at the corner is to change the boundary-layer thickness. The variable which controls the thickness is the density which decreases as the flow rounds the corner so that the boundary layer thickens. The calculated ratios of the thickness after expansion to thickness before expansion are given in the following table for representative free-stream Mach numbers:

M_o	2	4	6	8
Thickness ratio	2.1	4.0	6.0	7.6

An important consequence of the thickening at the corner is that the skin friction of the cylinder is small compared to that of the cone.

The skin-friction coefficients, calculated as outlined above, were found to be 25 to 30 percent lower than flat-plate results[4] for the air-off condition of the wind tunnel, and within 3 percent of flat-plate results for the air-on condition. This agreement with flat-plate results is surprising in view of the large differences from simple flat-plate conditions.

REFERENCES

Seiff, Alvin, James, Carlton S., Canning, Thomas N., and Boissevain, Alfred G.: The Ames Supersonic Free-Flight Wind Tunnel. NACA RM A52A24, 1952.

Mass. Inst. of Tech., Dept. of Elec. Engr., Center of Analysis. Tables of Supersonic Flow Around Cones, by the Staff of the Computing Section, Center of Analysis, under the direction of Zdenek Kopal. Tech. Rept. No. 1. Cambridge, 1947.

3. Chapman, Dean R.: An Analysis of Base Pressure at Supersonic Velocities and Comparison with Experiment. NACA TN 2137, 1950.

4. Clippinger, R. F., Giese, J. H., and Carter, W. C.: Tables of Supersonic Flow about Cone Cylinders. Rept. No. 729, Ballistic Research Laboratory, Aberdeen Proving Ground, July 1950.

5. Allen, H. Julian, and Nitzberg, Gerald E.: The Effect of Compressibility on the Growth of the Laminar Boundary Layer on Low-Drag Wings and Bodies. NACA TN 1255, 1947.

6. von Kármán, Theodore, and Tsien, Hsue-shen: Boundary Layer in Compressible Fluids. Jour. Aero. Sci., vol. 5, no. 6, April 1938.

7. Chapman, Dean R., and Rubesin, Morris W.: Temperature and Velocity Profiles in the Compressible Laminar Boundary Layer with Arbitrary Distribution of Surface Temperature. Jour. Aero. Sci., Sept. 1949, pp. 547-565.

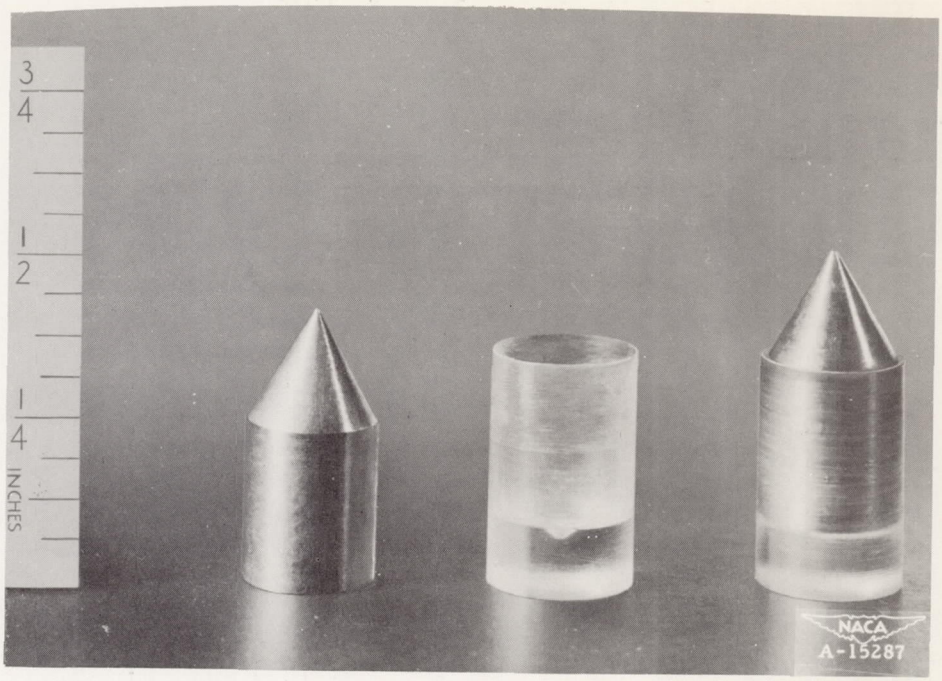

(a) Typical 60° cone cylinder and launching sabot.

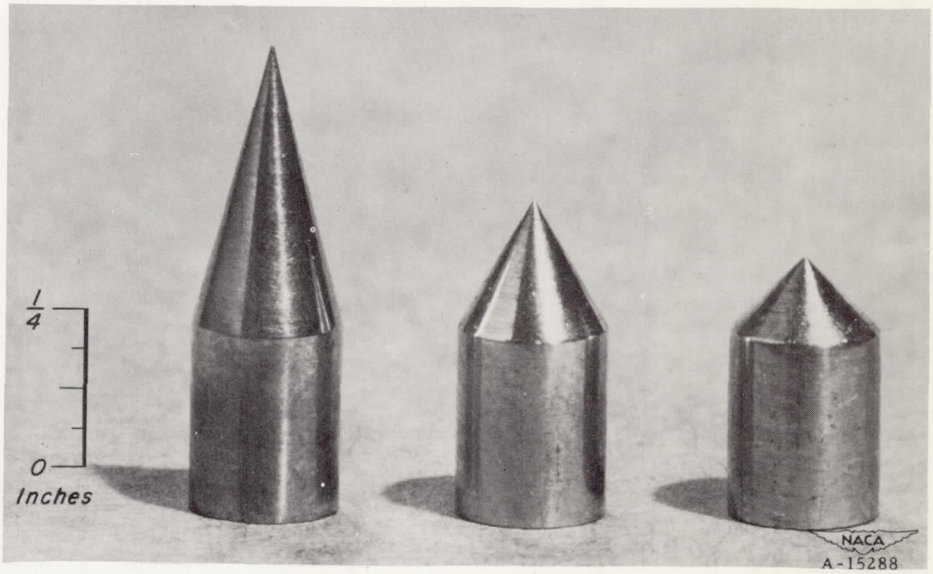

(b) Typical 30°, 60°, and 90° full-bore-diameter cone cylinders.

Figure 1.- Models.

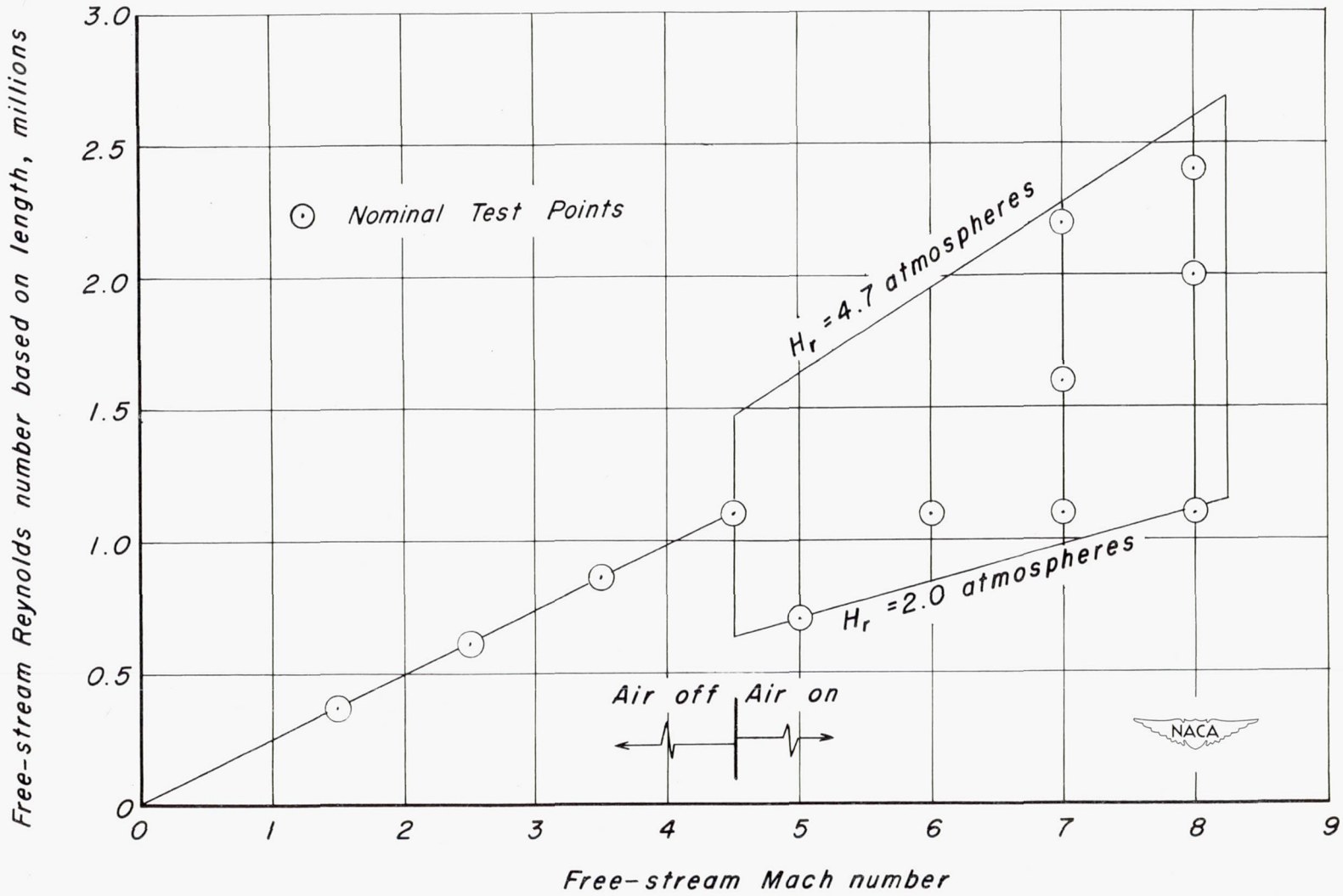

Figure 2.– Nominal test conditions for the smooth 60° cone cylinder.

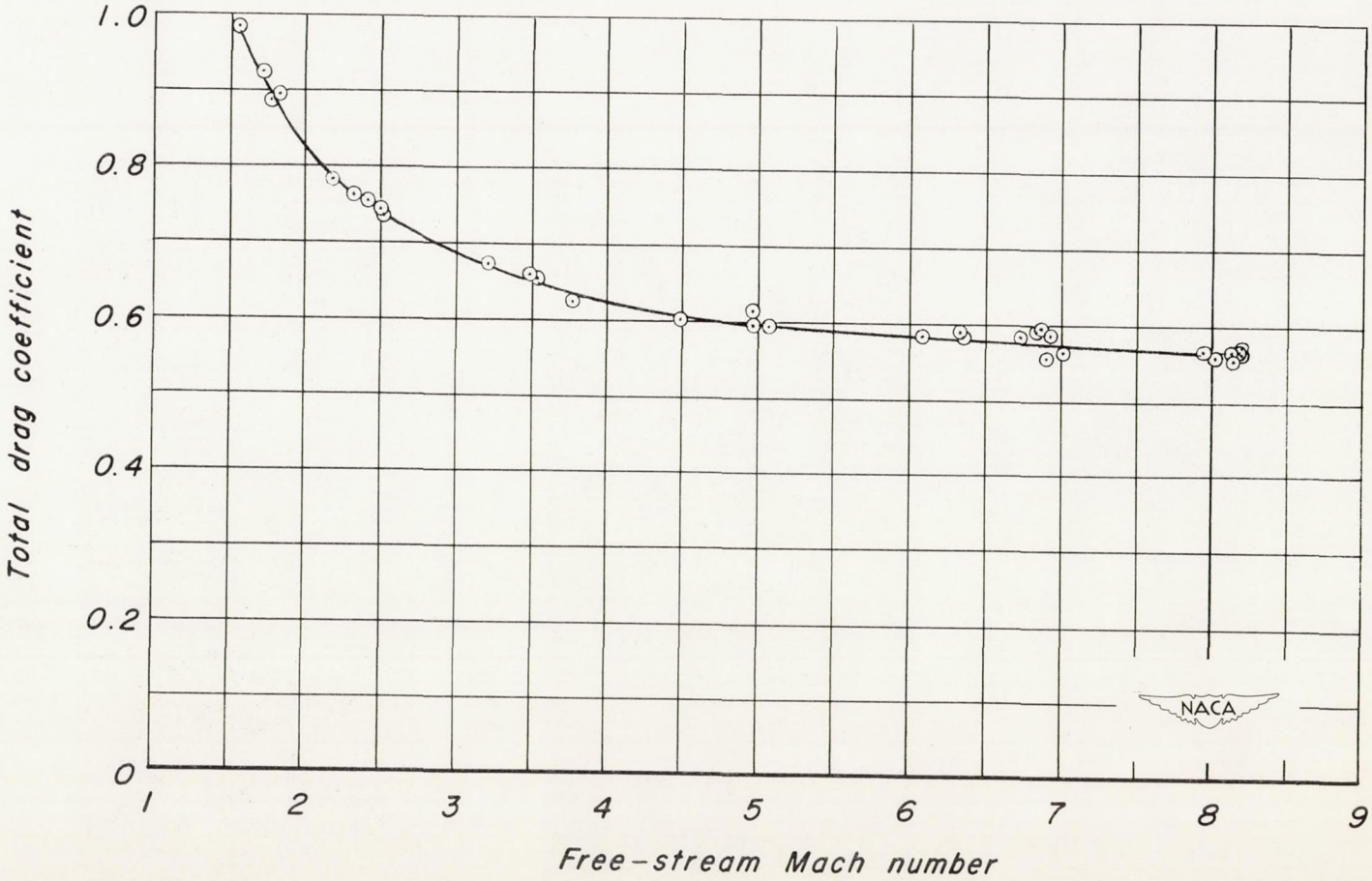

Figure 3.—Experimental variation of drag coefficient with Mach number for the smooth 60° cone cylinder.

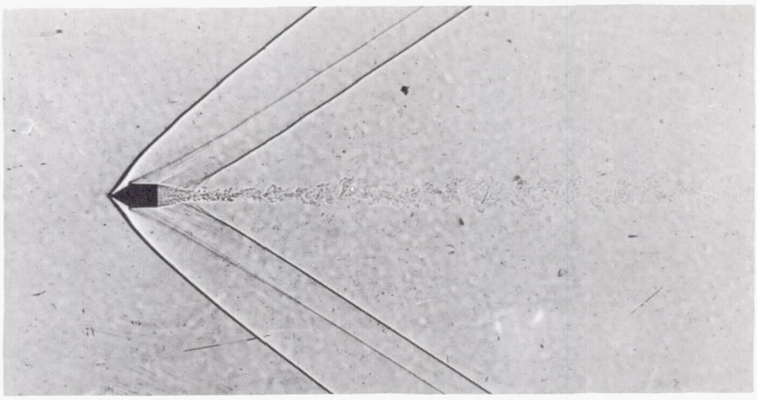

(a) M_o = 1.71, R = 430,000

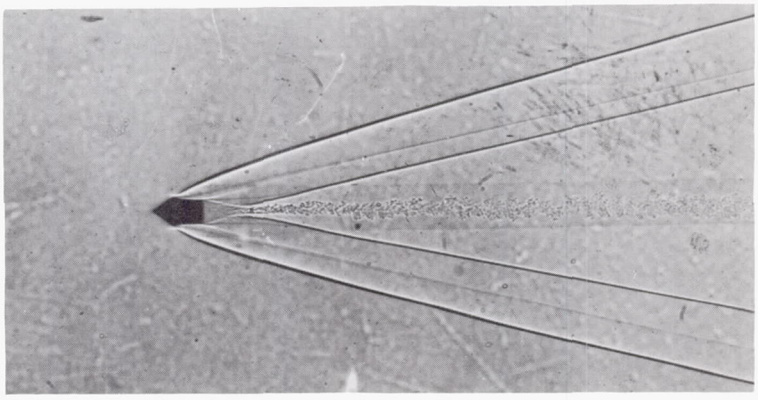

(b) M_o = 4.49, R = 1,140,000

(c) M_o = 8.14, R = 1,080,000

NACA
A-15927

Figure 4.– Shadowgraph pictures of the smooth 60° cone cylinder.

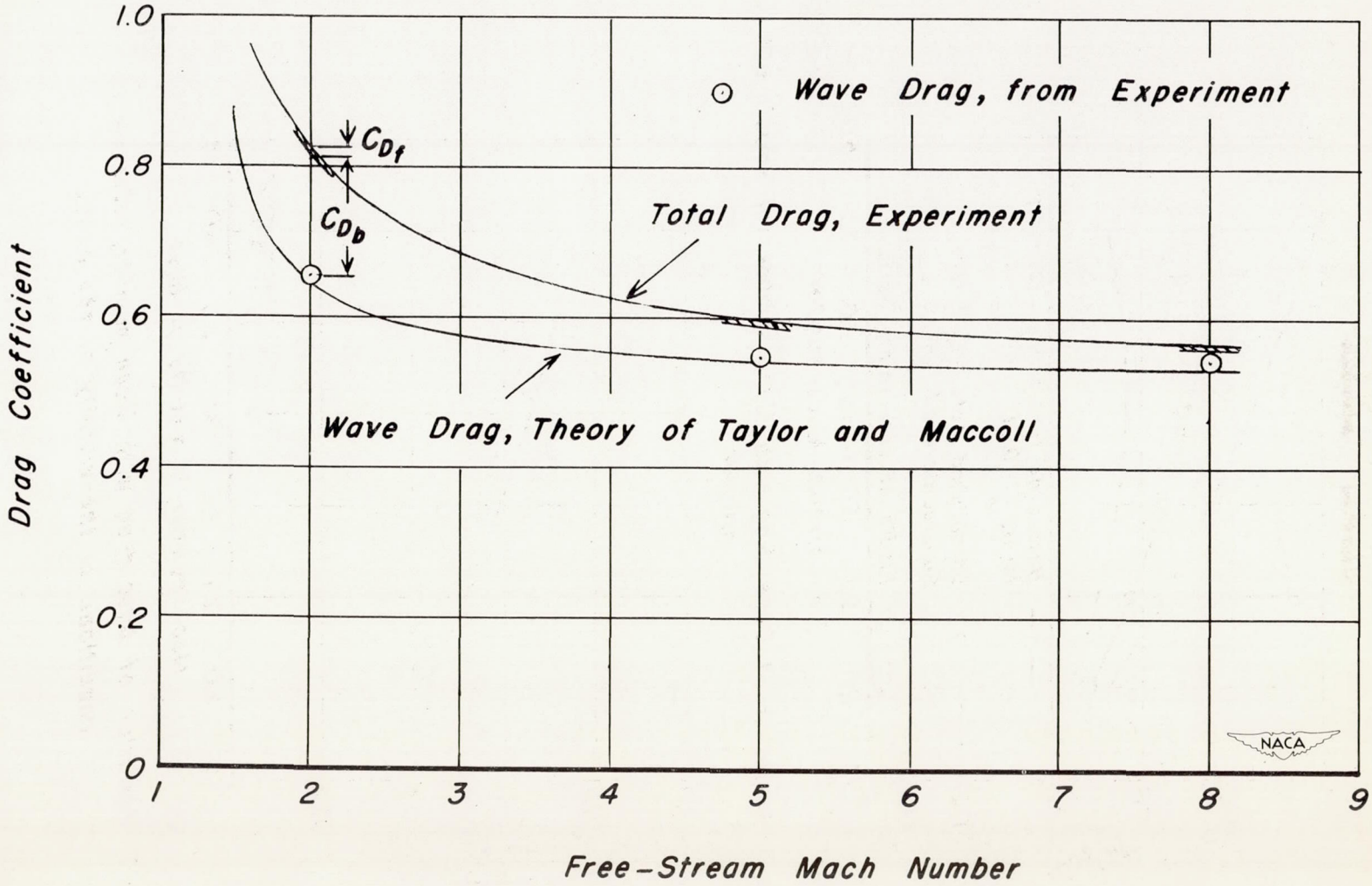

Figure 5.- Comparison with theory of Taylor and Maccoll.

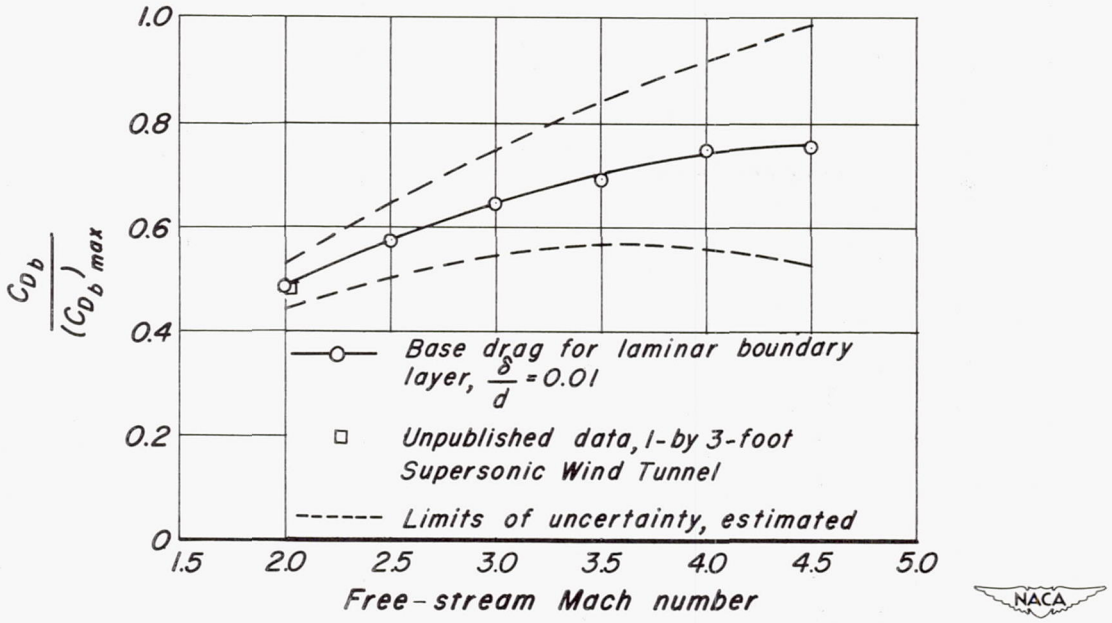

Figure 6.–Variation of base drag with Mach number for smooth 60° cone cylinder.

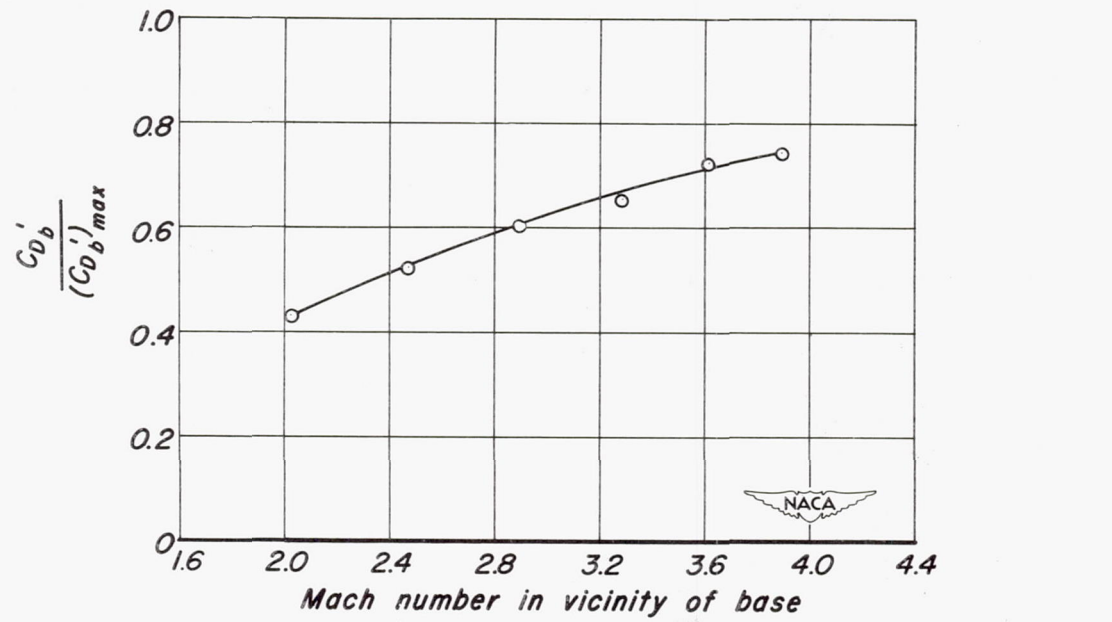

Figure 7.–Variation of base drag with Mach number, referred to conditions in the vicinity of the base.

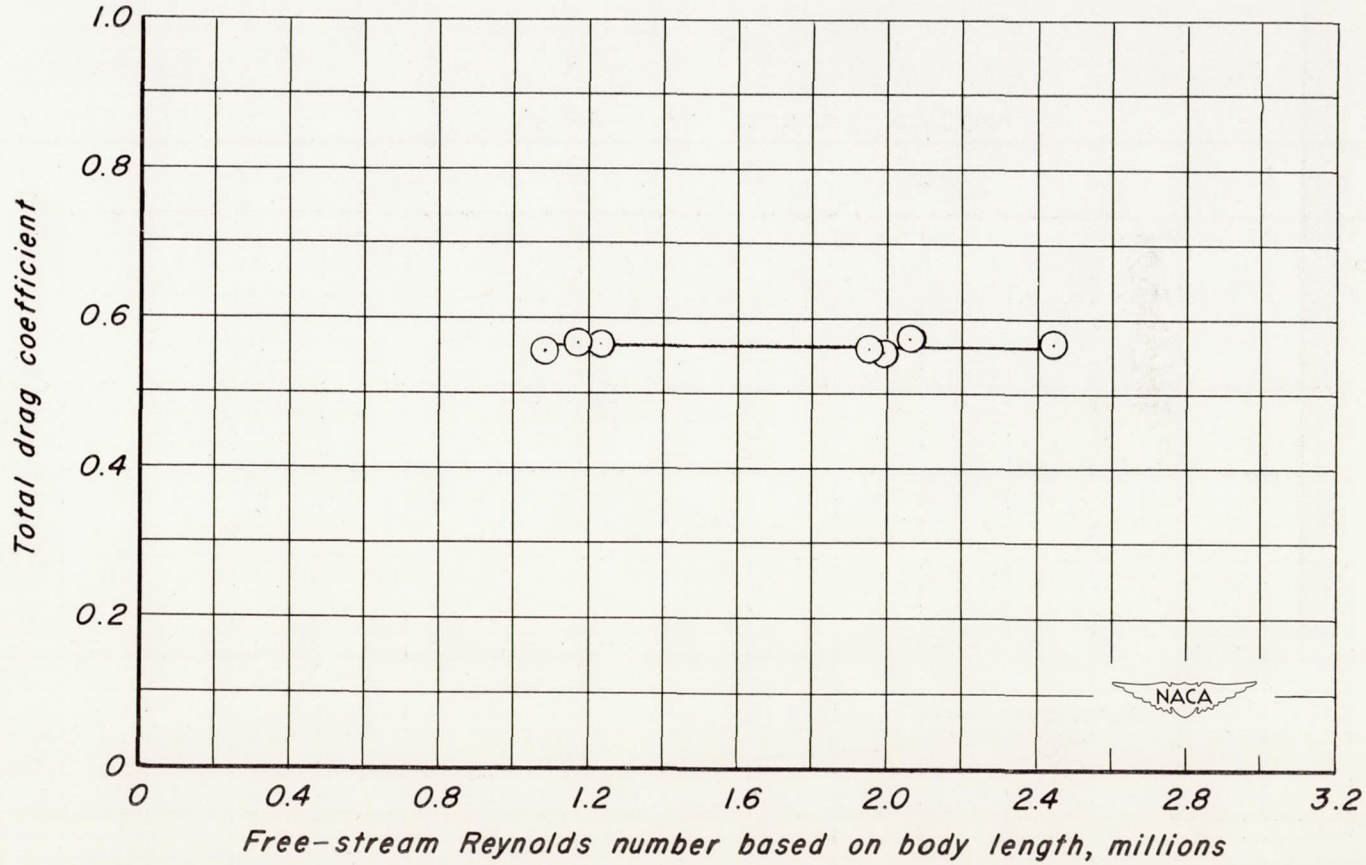

Figure 8.- The effect of Reynolds number on the total drag coefficient of the smooth 60° cone cylinder at Mach number 8.

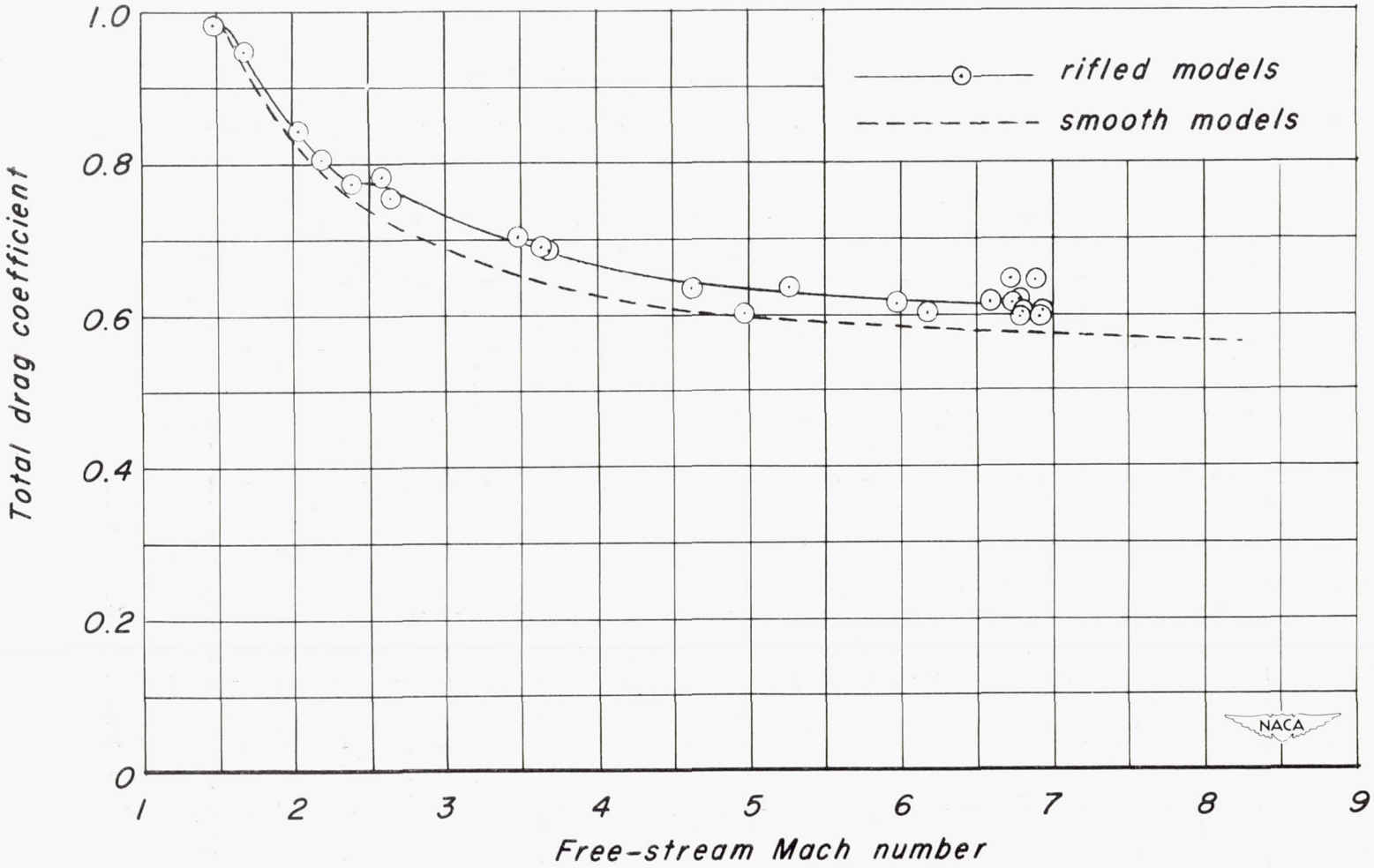

Figure 9.—Effect of rifling on total drag of 60° cone cylinder.

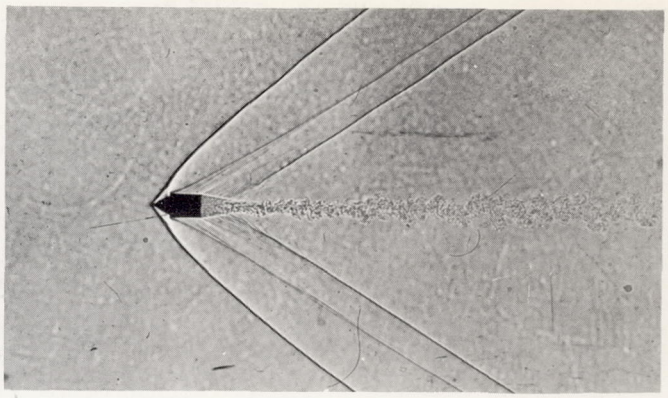

(a) M_o = 1.68, R = 460,000

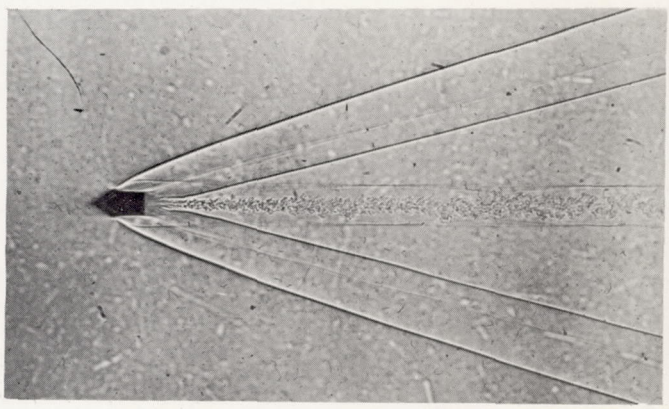

(b) M_o = 3.58, R = 970,000

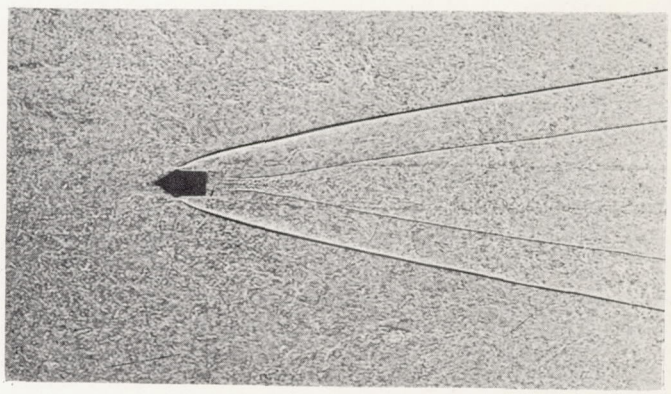

(c) M_o = 6.94, R = 1,090,000

NACA
A-16188

Figure 10.– Shadowgraph pictures of the rifled 60° cone cylinder.

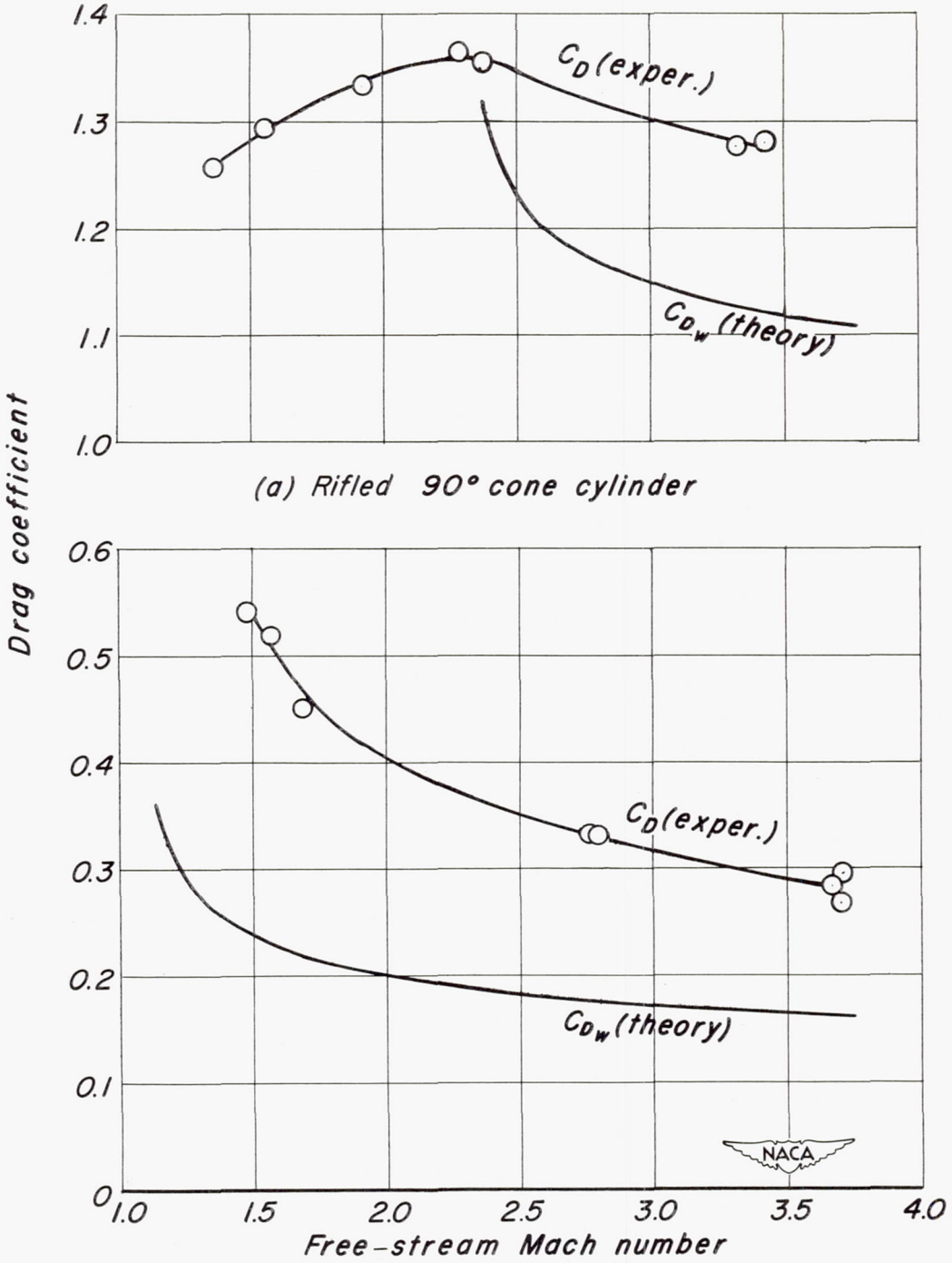

Figure 11.- Variation of drag coefficient with Mach number for the rifled 90° and 30° cone cylinders.

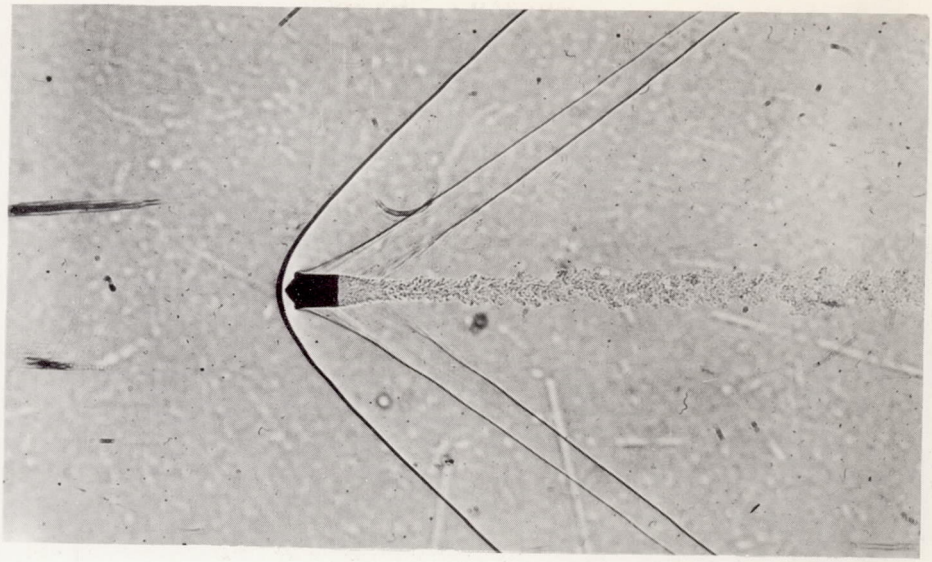

(a) M_o = 1.55, R = 350,000

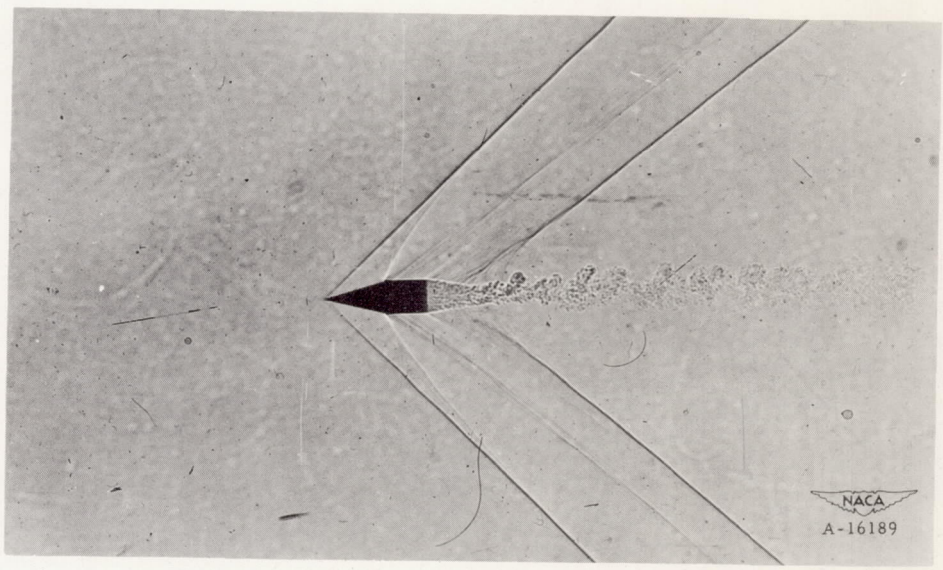

(b) M_o = 1.48, R = 600,000

Figure 12.– Shadowgraph pictures of the rifled 90° and 30° cone cylinders.

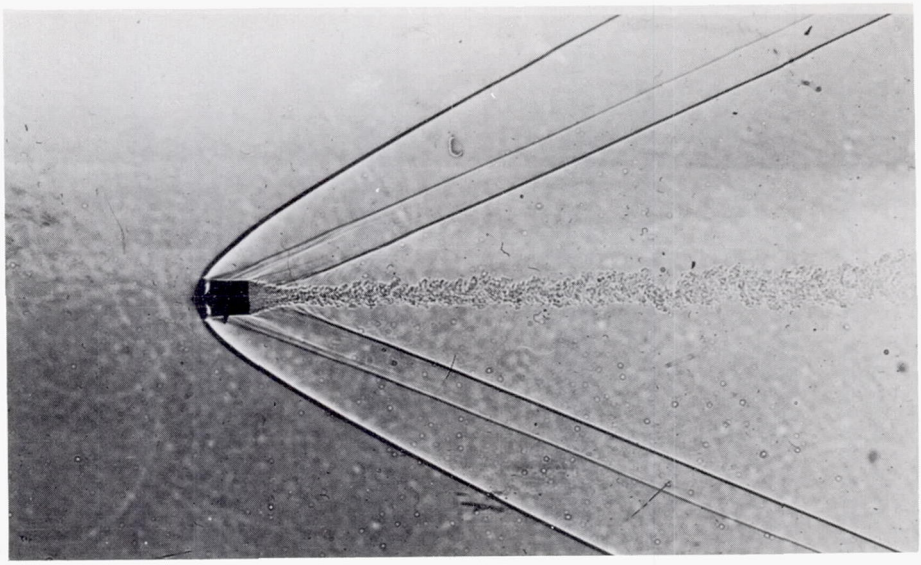

(c) M_o = 2.39, R = 530,000

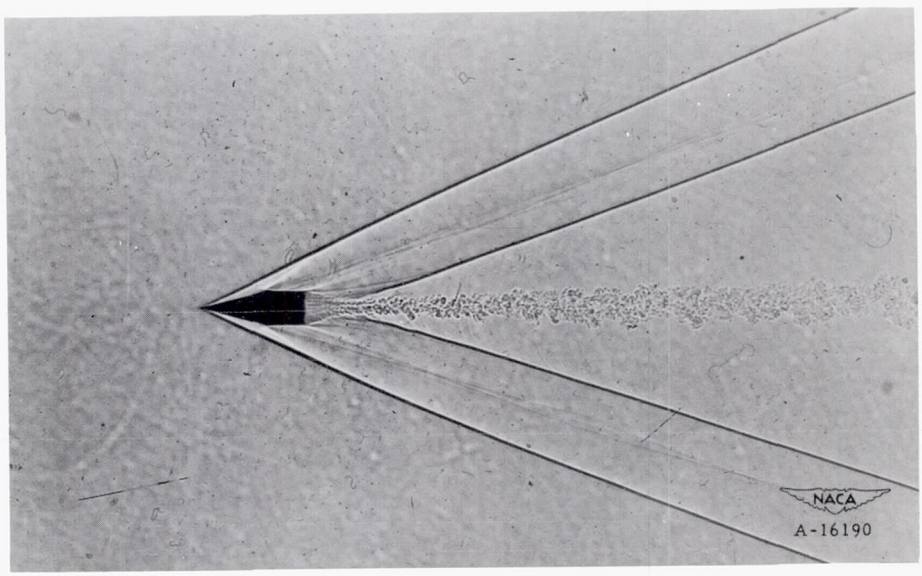

(d) M_o = 2.80, R = 1,140,000

Figure 12.– Continued.

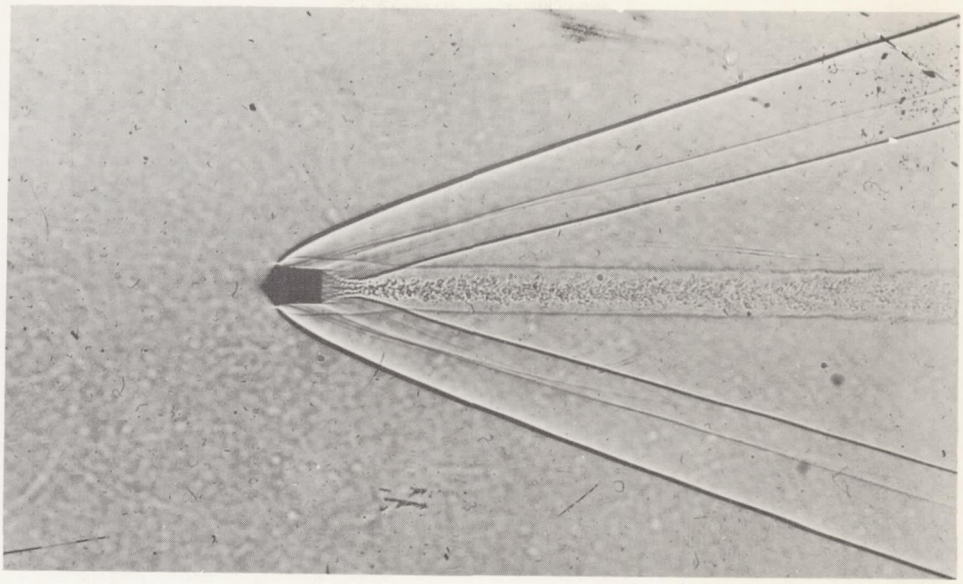

(e) M_o = 3.41, R = 950,000

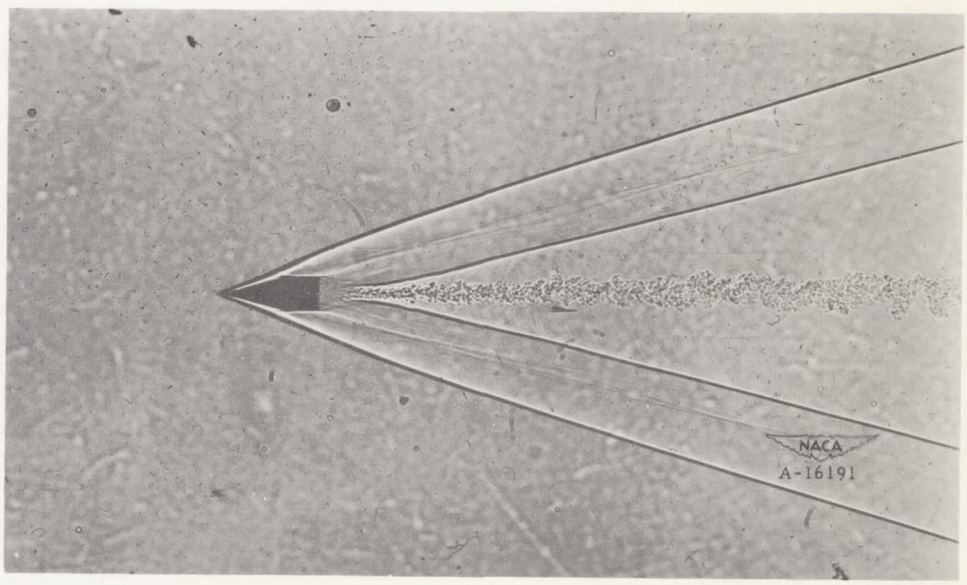

(f) M_o = 3.67, R = 1,450,000

Figure 12.– Concluded.